IEEE Access
Multidisciplinary ⋮ Rapid Review ⋮ Open Access Journal

Received 30 August 2022, accepted 14 September 2022, date of publication 20 September 2022,
date of current version 29 September 2022.

Digital Object Identifier 10.1109/ACCESS.2022.3208111

RESEARCH ARTICLE

Study on Wear of Electromagnetic Railgun

SHIDA REN[1], GANG FENG[2], AND SHAOWEI LIU[2]
[1]Graduate College, Air Force Engineering University, Xi'an 710051, China
[2]Air and Defense College, Air Force Engineering University, Xi'an 710051, China

Corresponding author: Shida Ren (timmyda@163.com)

This work was supported by the National Defense Science and Technology Fund under Grant 2201079.

ABSTRACT Sliding friction wear of high-speed current-carrying is a key factor limiting the engineering of electromagnetic railgun, and is also a hot spot and difficult area for current research. In this paper, we simulate the internal ballistic dynamics and electrical contact characteristics based on multi-physics field effects and consider the actual working conditions such as Lorentz force, friction force and interference fit to simulate the motion of the armature in the bore. Based on the Archard wear model, a finite element simulation method combining HyperMesh and ANSYS is proposed to realize the wear prediction. The simulation results are compared with the experimental results to verify the accuracy of the prediction model. The results show that under the single firing condition, the wear is mainly concentrated at the end of the armature arm, and the rail wear is relatively light; with the increase of electromagnetic thrust, the increase of armature wear volume does not change much and is approximately equal; the armature wear volume is influenced by the wear coefficient, in which the armature wear volume increases about 190 times when the wear coefficient increases from 1×10^{-6} to 1×10^{-3}. Therefore, in order to reduce the degree of wear between the armature and rails, the lubrication conditions should be improved as much as possible. This study provides a simulation method for the wear prediction of electromagnetic rail launcher, which is important for the engineering application of electromagnetic rail launcher.

INDEX TERMS Electromagnetic railgun, Archard wear model, frictional wear, finite element simulation, multi-physics field coupling.

I. INTRODUCTION

Electromagnetic railgun is an emerging weapon that can accelerate projectiles to ultra-high sonic velocities using electromagnetic forces [1], [2], [3]. This technology can break the limits of conventional powder velocity and precisely control the exit velocity of the projectile by controlling the pulse current [4], [5]. With its obvious advantages, electromagnetic rail launch technology has great potential for development in the military field [6].

During electromagnetic launch, there is a high speed, high current sliding electrical contact between the armature and the rails, which is a unique feature that distinguishes electromagnetic rail launchers from other conventional electromechanical devices. The ultra-high speed sliding of the armature in the fastened rail will inevitably cause wear of the armature and rail contact surfaces. Only a wear calculation model can be established to effectively suppress wear and improve the emitter service life [7], [8], [9], [10], [11], [12].

From the existing studies, there is less mature international experience on this problem and there is still a lot of work to be done. Lu *et al.* [13] analyzed the effect of temperature on inter-support rail wear by finite element simulation and found that as the temperature of the surface of the support rail increased, the elastic modulus and hardness of the contact material decreased and the inter-support rail wear increased; Singer *et al.* [14] studied a solid lubricating interface compound (SLIC) for the protection of low-speed railguns. The results showed that the compound coating effectively mitigated armature arcing and frictional wear; Wu *et al.* [15] analyzed and calculated the ballistic dynamics, frictional failure and nonlinear electrical contact inside the armature based on multi-physical field effects and verified the results experimentally; Bansal *et al.* [16] conducted frictional wear tests of sliding electrical contact between copper alloy and aluminum alloy by friction testing machine. It was found that the contact

The associate editor coordinating the review of this manuscript and approving it for publication was Guido Lombardi.

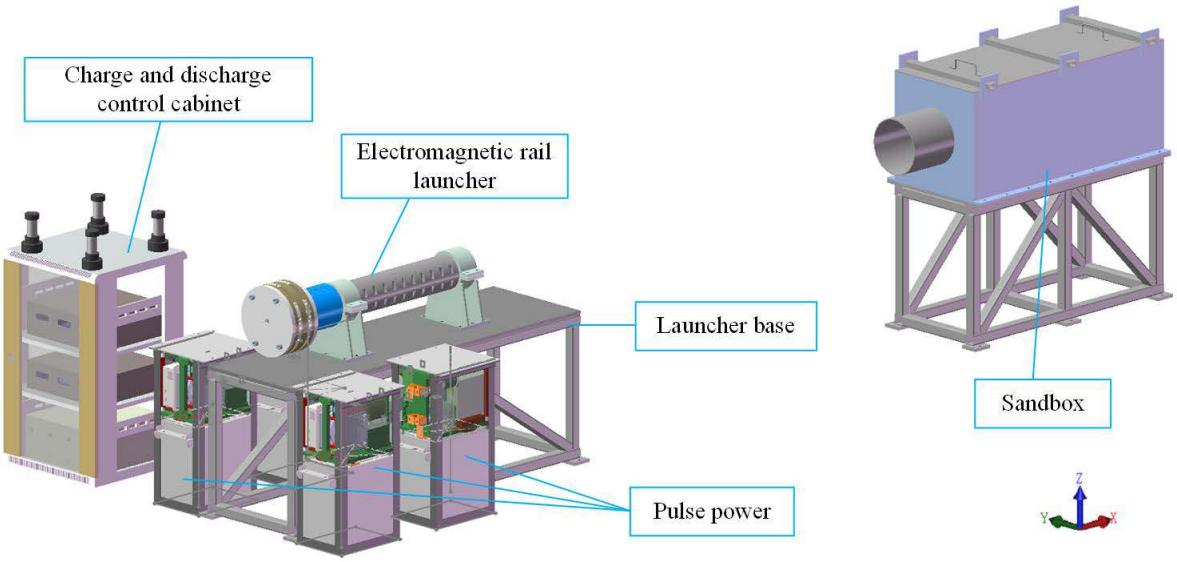

FIGURE 1. Electromagnetic launch system.

area and wear diameter increased with the increase of current; Gao *et al.* [17] used finite element simulation method to simulate the wear characteristics, but the distribution of wear amount was not obtained. The methods and conclusions of the above studies are important references for the subsequent research on the wear of electromagnetic rail launchers, but there is still a lack of effective simulation means to reduce the test cost.

In this paper, the internal ballistic dynamics of the contact surface is simulated considering the frictional resistance and nonlinear electrical contact. Based on the wear mechanism of the four-rail electromagnetic launcher, the frictional wear of the armature and rail contact surface during the electromagnetic launch process is simulated by the finite element method using the Archard wear model, combined with the platform characteristics and actual loading conditions of the four-rail electromagnetic launcher, and the wear distribution of the armature armature with the armature morphology of the launch test is The wear distribution of the armature arm is compared with the armature shape of the launch test. The wear mechanism of the electromagnetic rail launcher is proposed according to the characteristics of the ultra-high speed current-carrying sliding. Finally, the effects of electromagnetic thrust and wear coefficient on the wear characteristics are analyzed.

II. ELECTROMAGNETIC LAUNCH SYSTEM ANALYSIS

The electromagnetic launch system is composed of pulse power supply, charge and discharge control cabinet, electromagnetic rail launcher, sandbox and launcher base. The electromagnetic emission system is shown in the Figure 1.

The pulse power supply quickly converts the kinetic energy stored in the rotor into electrical energy through high-speed rotation, and the output current can reach millisecond MA, which can meet the high power requirements of electromagnetic launch; the charge drain control box is used for discharging the capacitor after the pulse power supply is finished, which is the safety protection subsystem of the pulse power supply; the electromagnetic rail launcher is used for the launch of the projectile; the sand box is mainly used for the recovery of the armature; the launcher base is mainly used for carrying launcher.

The pulsed power supply uses eight 2000 uF power modules, and the power supply uses a voltage of 3.3 kV and a 5 μH inductor to adjust the waveform. The current waveform diagram of the pulsed power supply and the local magnification diagram within 0∼0.5 ms are shown in Figure 2. The current amplitude rises rapidly from 0 A in a very short period of time and continues to decay after reaching a peak of 400 kA at the 0.2 ms moment. The current amplitude drops abruptly at the 3.4 ms moment, when the armature is discharged. Due to the limitation of simulation conditions, the wear analysis of the complete firing process is not possible at present, so this paper only simulates the motion and wear situation in the time period of 0∼0.5 ms.

Corresponding to the current waveform, the electromagnetic thrust, armature velocity and displacement curves with time are shown in Figure 3. As can be seen from the figure, the electromagnetic thrust reaches a maximum value of 1258388.61 N at 0.2 ms, and then decreases to 517838.27 N. The armature accelerates to 404.6 m/s at 0.5 ms under the excitation of the high pulse power supply, and the maximum sliding distance can reach 0.104 m. The internal ballistic motion characteristics obtained in this section will lay the foundation for the subsequent study of wear characteristics.

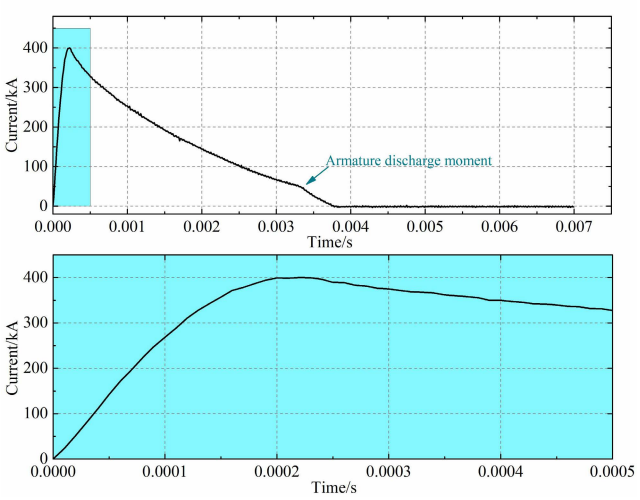

FIGURE 2. Current waveform diagram.

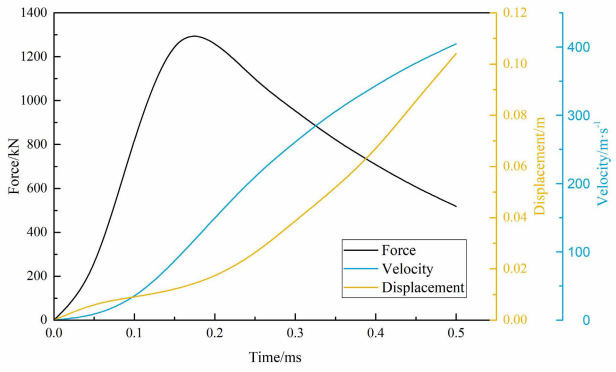

FIGURE 3. Curves of electromagnetic thrust, armature velocity and displacement versus time.

III. CONTACT CHARACTERISTIC ANALYSIS

The contact characteristics, i.e. the size of the contact area between the armature and the rail and the stress distribution in the armature, are important factors in determining the armature performance, and are also the main cause of frictional wear formation. In order to better understand the mechanism of wear generation, this section investigates the contact characteristics during transient launch.

A. SIMULATION MODEL

The physical diagram of the electromagnetic transmitter is shown in Figure 4(a). The armature and rails models are constructed based on the solid structure and parameters as shown in Figure 4(b).

The four rails are distributed in a 90° circular array around the armature, with an emitter diameter of 24 mm × 24 mm, a rail length of 890 mm, and an armature overfill of 0.14 mm. After measurement, the volume of the armature is 9934.8 mm^3 with a mass of 27.52 g; the volume of one rail

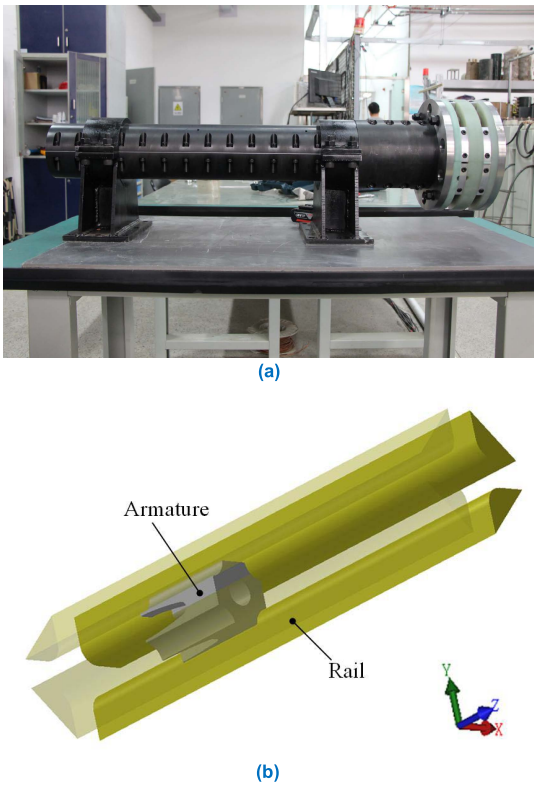

FIGURE 4. Armature and rails model. (a) Electromagnetic launcher test platform; (b) Armature and rails structure.

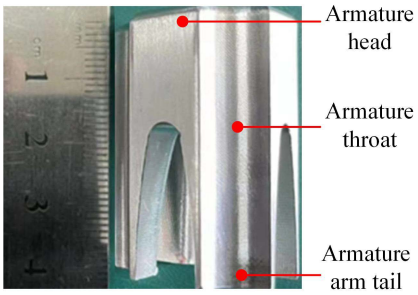

FIGURE 5. Armature structure.

is 1.09 × 10^5 mm^3 with a mass of 0.905 kg. The physical diagram of the armature studied in this paper is shown in Figure 5.

B. ANALYSIS OF SIMULATION RESULTS

As a key component of the electromagnetic rail launcher, the condition index of the armature has an important impact on the launch process. In order to ensure the high-speed current-carrying sliding performance of the armature in the gun chamber, an interference fit is used between the armature and the rail. Therefore, after the armature is assembled, the contact surface between the armature and the rail will generate preload and deformation. By the finite element simulation method, the contact state (contact state at the

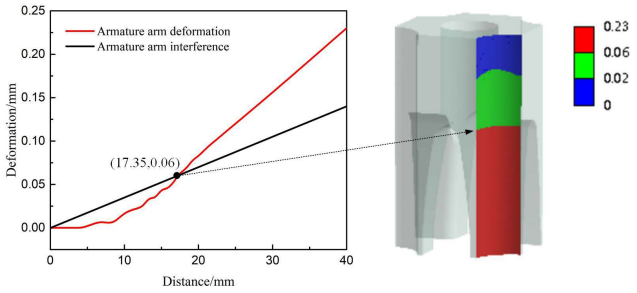

FIGURE 6. Armature arm deformation diagram.

moment of 0) after armature assembly is obtained as shown in Figure 6.

The analysis in the figure shows that after the interference assembly, the maximum deformation of the armature arm is 0.23 mm, which is larger than the interference amount of 0.14 mm. From this, it can be seen that there is a gap between part of the armature arm and the rail. When the deformation variable of the armature arm is equal to the interference amount at this position, the contact between the armature and the rail just occurs, that is, at the intersection of the two curves in Figure 6. And in the area where the armature arm shape variation is greater than 0.06 mm (the red area in the cloud diagram), separation of the armature from the rail occurs. The blue and green areas are in close contact.

During the launch process, the armature makes direct contact with the orbit to induce a pulsed current to excite the magnetic field, and the armature is accelerated by the electromagnetic force. The armature arm is expanded outward by the Lorentz force, resulting in an increase in the contact pressure between the armature and the rails, and the contact pressure changes with time. Using the coupled electromagnetic-structural field simulation method, the contact pressure clouds at different moments are obtained as shown in Figure 7.

As can be seen from the figure, the distribution of contact pressure is affected by the curved surface, showing a butterfly-wing distribution and mainly concentrated in the armature throat, indicating that the armature arm starts to bend at the armature throat. The analysis shows that the current is on the rising edge from 0-0.02 ms, so with the increase of time, the Lorentz force gradually increases and the armature arm flares out, resulting in the contact pressure between armature and rail gradually increases, and the maximum contact pressure can reach 1067.6 MPa at 0.02 ms; the contact pressure increases with the increase of time, and the contact area gradually spreads from the armature throat to the tail of armature arm.

IV. WEAR CHARACTERISTIC ANALYSIS

Tribological behavior is related to the behavior of the whole system, which is not only between materials, and tribological wear of materials cannot be defined without the action of the complete system [18]. Therefore, during the frictional wear

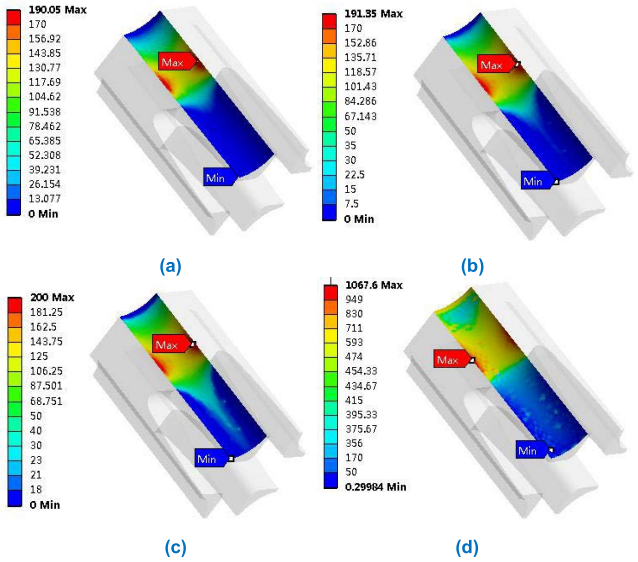

FIGURE 7. Equivalent force cloud at different moments: (a) 0.005ms; (b) 0.01ms; (c) 0.015ms; and (d) 0.02ms.

study of electromagnetic launchers, the wear behavior needs to be analyzed in the context of the entire emitting system. Wear simulations and tests with reasonable extrapolation of the results are extremely necessary for the study of wear damage and potential wear mechanisms of electromagnetic launchers.

Persad and Castro [19] performed a microscopic analysis of the orbit after electromagnetic launch and the observations showed that aluminum residues were present from the start position of the orbit, which could prove the presence of melting and material loss of the armature during the launch process, from which it can be judged that the main form of wear occurring on the electromagnetic orbital launcher is adhesive wear [20]. The Archard wear model can be used for effective prediction of adhesive wear. In this section, the wear characteristics of the electromagnetic rail launcher are simulated based on the Archard wear model; then the simulation results are compared with the wear profiles after the launch test to verify the accuracy of the simulation method; finally, the influence law of two parameters, electromagnetic thrust and wear coefficient, on the wear characteristics is analyzed.

A. ARCHARD WEAR CALCULATION MODEL

The contact surface between the armature and the rail is machined so that the surface is in a relatively smooth state on a macroscopic level. However, the frictional contact surface is not flat at the microscopic level. When the two are in contact, they are actually in point contact. At this point, a load is applied between them and the two move relative to each other [21]. Under local stress, the contact area is sheared or even deformed, and the atoms between the internal metallic materials are transferred and bonded under external forces,

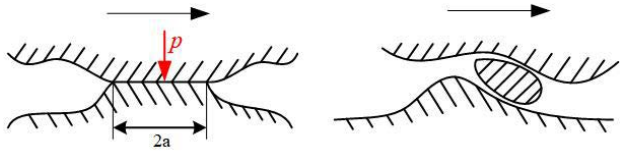

FIGURE 8. Schematic diagram of adhesive wear model.

resulting in the occurrence of adhesion. This kind of wear is adhesive wear. The adhesive wear model is shown in Figure 8.

Assume that there are u convex peak elements on the unit contact surface, and under the action of pressure p, the peak elements in contact form a bonding point with a radius of a. σ_{SC} is the yield limit of softer materials. At this point, the material at the bonding point is in a state of yield. The compression yield limit is

$$p = u \cdot \pi a^2 \sigma_{SC} \tag{1}$$

Due to the relative motion, some of the adhesion points separate from the softer material. Assume that the probability of adhesion point separation per unit area is k and the wear of contact surface per unit area is.

$$dV = k \cdot u \cdot \frac{2}{3}\pi a^3 \tag{2}$$

In general, for elastic materials, $\sigma_{sc} \approx H/3$, H is the Brinell hardness.When the sliding displacements are $2a$, the wear per unit displacement is:

$$\frac{dV}{dl} = k\frac{u \cdot \frac{2\pi a^3}{3}}{2a} = \frac{kup}{3\sigma_s} = K\frac{p}{3\sigma_s} \tag{3}$$

Based on the above study, the calculation equation of the Archard wear model embedded in the finite element simulation software ANSYS is as follows.

$$\begin{cases} dV = K\dfrac{p \cdot dl}{H} \\ \omega = \dfrac{dV}{dt} = \dfrac{Kp^n \boldsymbol{v}_s^m}{H}\boldsymbol{n} \\ h = \displaystyle\int_0^t \frac{V(t)}{A(t)}dt = \frac{K}{H}\int_0^t \frac{p \cdot v_s(t)}{dA}dt \end{cases} \tag{4}$$

where ω is the wear rate, in mm^3/s; V is the wear volume, in mm^3; H is the material hardness of the softer material, in Pa; p is contact pressure, unit N; $\boldsymbol{v_s}$ is the sliding velocity, in m/s; m and n is velocity exponent and pressure exponent respectively; $\boldsymbol{n}$ is the in-plane normal direction.

B. SIMULATION CONDITION SETTING

The solution of the wear process is a nonlinear problem, which cannot be solved directly for wear in the integration module. It is necessary to write an APDL command flow program to customize the intrinsic parameters of the Archard wear model. The parameters correspond as shown in Table. 1.

Based on the actual lubrication of the four-rail electromagnetic launcher armature and guide rail, the C1 parameter for this simulation test was determined to be 1×10^{-3}; parameter C2 was set to the hardness of the aluminum alloy material; parameters C3 and C4 were set to 1, i.e., the contact pressure and relative motion speed generated by the actual load applied during the simulation were used; the control term coefficient C5 was set to 0, i.e., the contact pressure was used in the wear calculation to further control the implementation of the Archard model. Since all material parameters can be a function of temperature, the effect of temperature on wear is considered in solving for wear.

TABLE 1. Command parameters.

Parameter	Meaning	Numerical value
C1	Wear coefficient (k)	1×10^{-3}
C2	Material hardness (H)	120
C3	Contact pressure index (m)	1
C4	Relative velocity index (n)	1
C5	Control item	0

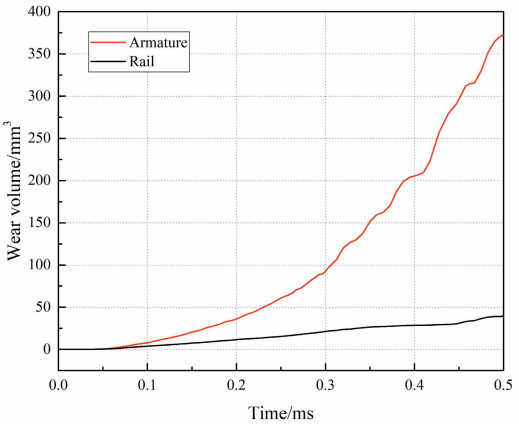

FIGURE 9. Armature and rail wear volume change curve.

A contact pair is set up between the armature and the rail. To prevent contact unit penetration, an enhanced Lagrangian algorithm is used and nodal contact is employed as a detection method. The contact surfaces of the two entities are set as contact body and target body, and the contact surface set as target body is examined for wear.

The process of wear will cause the missing of mesh cells, so it is necessary to perform mesh update after each time step calculation to adapt to the next iteration of wear calculation to correct the mesh deformed by wear and ensure the condition of the next iteration calculation is satisfied. The adaptive mesh is set up using the APDL program and the adaptive parameter is set to 50%; the analysis step length is taken as 0.01ms, which is consistent with the kinetic analysis step length.

C. ANALYSIS OF WEAR SIMULATION RESULTS

Based on the User Defined Result wear calculation method, parameters such as wear volume and wear rate of the contact surface can be evaluated. The expression relation

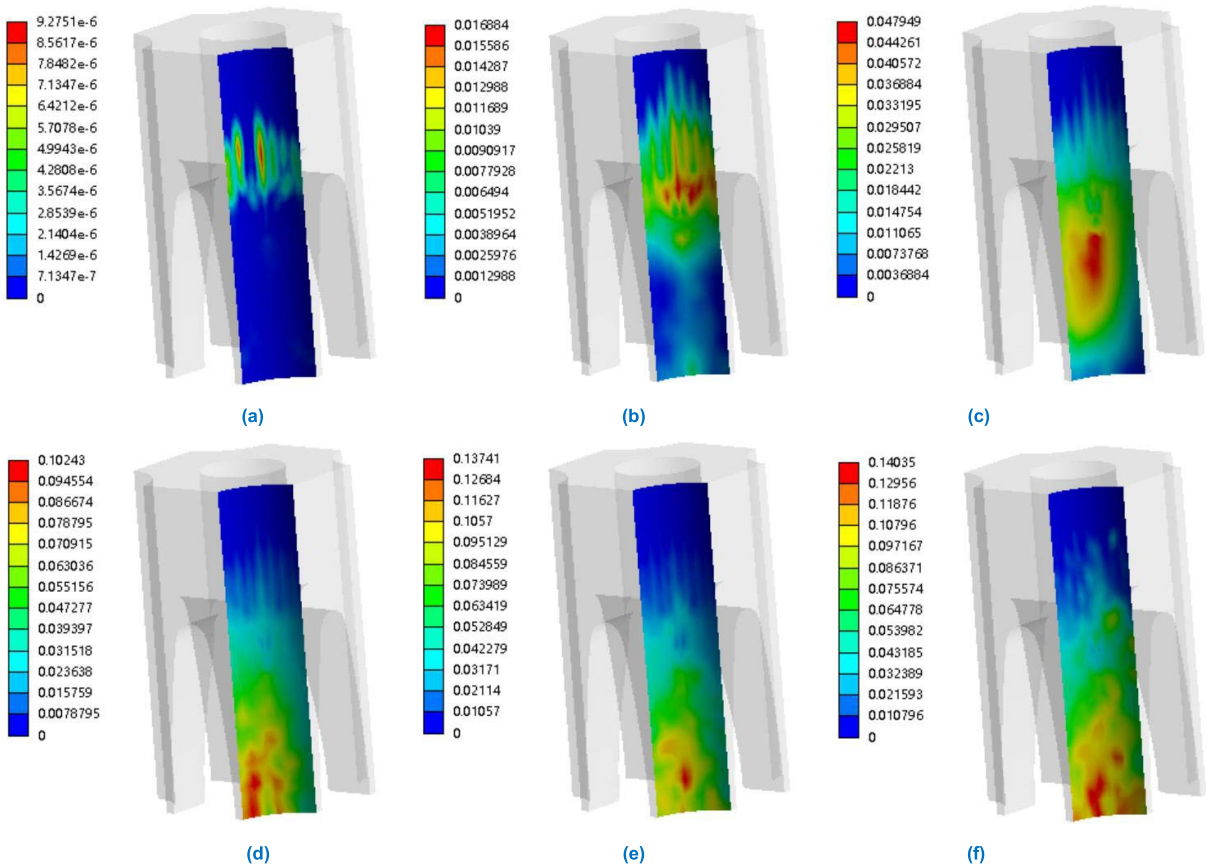

FIGURE 10. Cloud of armature arm wear volume at different moments: (a) 0.005ms; (b) 0.01ms; (c) 0.015ms; (d) 0.3ms; (e) 0.4ms; and (f) 0.5ms.

contnmisc189 is defined to simulate the wear profile of the contact surface mesh cell. Here the wear rate is defined as the wear volume per unit time. The pivot rail wear volume variation curve with firing time is shown in Figure 9.

From the figure, it can be seen that the wear mainly occurs on the surface of the softer material, and the armature surface wear is serious, while the copper rail surface wear is relatively mild. At the moment of 0.5ms, the armature wear volume is 372.83 mm^3; the rail wear volume is 39.35 mm^3, and the armature wear phenomenon is more significant. Under the same conditions, the armature wear volume is about 10 times that of the orbit after a single launch. Therefore, for the convenience of measurement and observation, the armature is chosen as the object of the wear characteristics study in the following. The wear volume cloud of armature arm at different moments is shown in Figure 10.

From the figure, it can be seen that the wear mainly occurs at the armature throat at the beginning of the launch, and the wear area gradually shifts from the armature throat to the tail of the armature arm as time increases, which is consistent with the distribution of the contact pressure over time. This is because at the beginning of firing, the contact pressure at the armature throat is the highest, and the armature arm tail is separated from the rail. With the increase of pulse current, the armature arm undergoes outward expansion, which puts the armature arm under a larger load. At the same time, influenced by the principle of shortest path of current and skin effect of current, the armature arm tail generates current concentration and then generates a large amount of heat at the armature arm tail, which causes the armature material near it to fall off rapidly, so the armature arm tail wears the most strongly, which is consistent with the Archard wear theory.

D. ELECTROMAGNETIC LAUNCH TEST

This test was conducted to verify the correctness and feasibility of the wear simulation method for the electromagnetic rail launcher by comparing the simulated and tested armature wear patterns. The parameters of the pulsed power supply used for the launch test are shown in Section II. Figure 11 shows the photographs of the electromagnetic rail launch system before launch, the instant of armature discharge and the instant of armature injection into the sandbox.

The state in the gun chamber was photographed using an endoscope after firing, and the rails state after firing is shown in Figure 12(a). The state of the armature contact surface after the end of firing is shown in Figure 12(b).

It can be seen from the photos that the rail and armature are covered by obvious wear and ablation. By comparing the

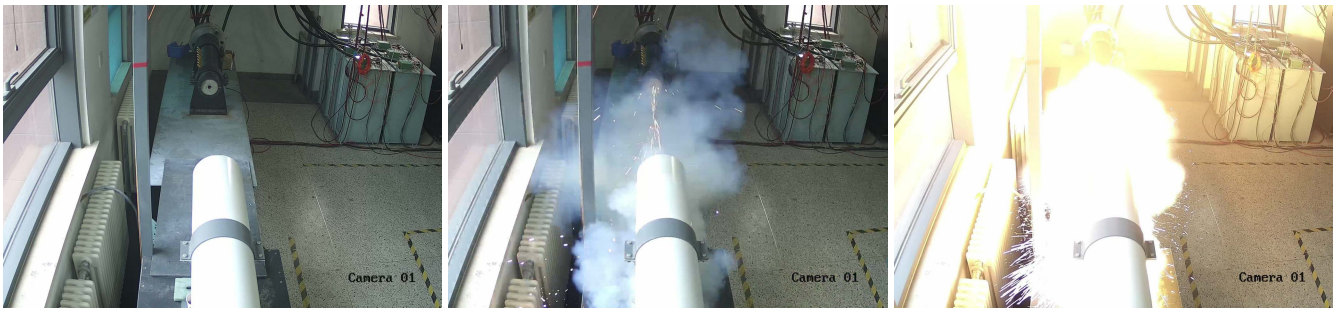

FIGURE 11. Electromagnetic launch process: (a) Schematic diagram of the electromagnetic rail launch system before firing; (b) the moment of armature discharge; and (c) the moment of armature injection into the sandbox.

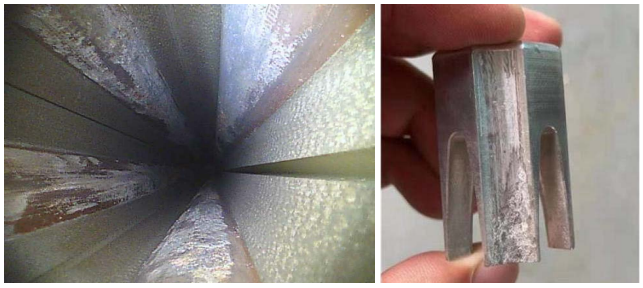

FIGURE 12. Armature and orbital status after launch: (a) Rails Status; and (b) Armature status.

armature arm wear simulation with the launch test, the wear pattern of the armature arm is basically the same. The wear on the armature head is slight while the wear on the armature tail is the most severe. The correctness and feasibility of the wear simulation method and the conclusions obtained were verified.

E. ANALYSIS OF FACTORS INFLUENCING WEAR CHARACTERISTICS

1) EFFECT OF ELECTROMAGNETIC THRUST ON WEAR CHARACTERISTICS

During the electromagnetic emission, the electromagnetic thrust is different, then the power discharge waveform is also different, which will lead to the subsequent change of Lorentz force, then the lateral squeezing force between the pivot rails is changed. In order to control the variables uniquely, only the electromagnetic thrust is changed without changing the pivot rail contact. The variation curves of armature wear volume for the conditions of electromagnetic thrust of 20,000 N, 30,000 N, 40,000 N and 50,000 N are shown in Figure 13(a). The speed variation curves with time for different electromagnetic thrusts are shown in Figure 13(b).

From the figure, it can be seen that the wear rate increases with the increase of electromagnetic force, but the wear rate varies under different electromagnetic thrusts. When the electromagnetic thrust is 20,000 N, the growth rate of wear volume with time does not change significantly, and the

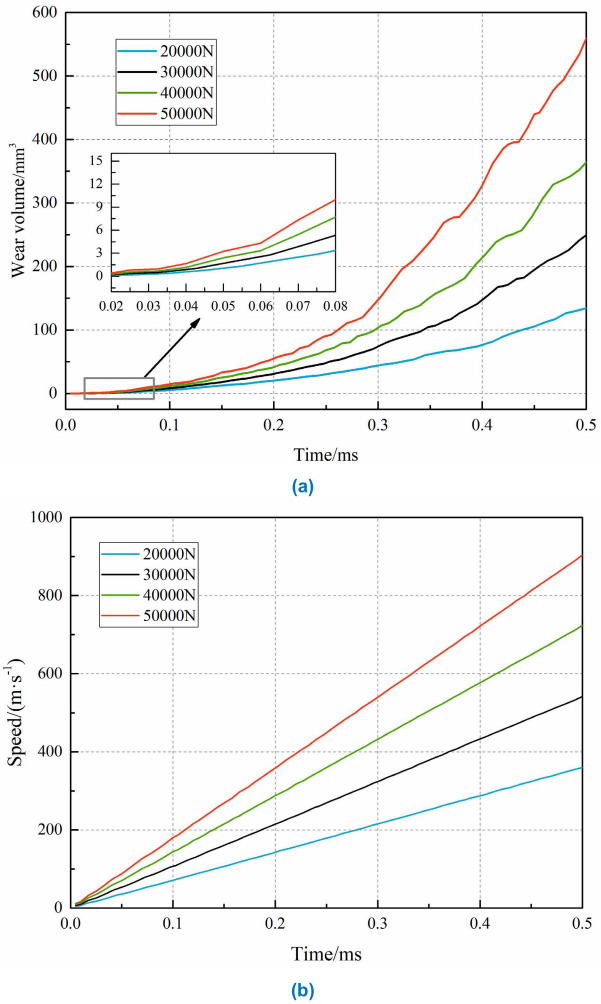

FIGURE 13. Effect of electromagnetic thrust on wear characteristics: (a) Variation of wear volume with time; and(b) Variation of speed with time.

armature wear volume reaches 134.36 mm^3 at the moment of 0.5ms armature movement; when the electromagnetic thrust is 30,000 N and 40,000 N, the maximum wear volume is 249.55 mm^3 and 364.15 mm^3 respectively; when the

electromagnetic thrust is 50,000 N, the The wear rate gradually increases with time, showing exponential growth, and the wear volume reaches 559.41 mm^3 after 0.5 ms of launch. with the equal proportional increase of electromagnetic thrust, the increase of wear volume does not change much.

The wear volume distribution in the time domain was obtained by analyzing the variation law of the wear volume with time for different electromagnetic thrusts. However, in the process of changing only the electromagnetic thrust, the armature motion acceleration and velocity also change. In order to get the distribution of wear volume in the spatial domain, the change of armature motion velocity with time under different electromagnetic thrusts needs to be analyzed. From Figure 13(b), it can be seen that the armature slides with a certain acceleration under different electromagnetic thrusts, which shows a proportional correlation with the increase of wear volume under different electromagnetic thrusts. After reaching the peak current moment in Figure 13(a), the wear volume change curve for a period of time is locally enlarged and combined with the velocity curve observation, it can be seen that the armature start-up period is before the 0.02ms moment, the armature velocity is almost 0, and the armature wear volume is extremely small at this time. Therefore, the electromagnetic thrust affects the acceleration of armature movement, because the power discharge time is certain, if the generated electromagnetic thrust is too small, after the power discharge is over, the armature does not slide off the rail, which will affect the launch timing or even damage the electromagnetic launch device; if the electromagnetic thrust is too large, the armature movement speed is too high, which will aggravate the armature and rails wear and even the phenomenon of turning.

2) INFLUENCE OF WEAR COEFFICIENT ON WEAR CHARACTERISTICS

The wear coefficient responds to the smoothness between the contact surfaces. In order to study the effect of the wear coefficient on the wear volume, this section adopts the 0.14mm overload pivot rail model and applies the flat-top wave current excitation shown in Figure 2, then the electromagnetic thrust acting on the armature is shown in Figure 3. The wear coefficients K are set as 1×10^{-3}, 1×10^{-4}, 1×10^{-5}, and 1×10^{-6} respectively, and the four coefficients correspond to four different smoothness degrees between the pivot rails, and all other conditions are the same, and the firing process is simulated separately. The variation curves of armature wear volume with time for different wear coefficients are shown in Figure 14(a). The velocity versus time curves for different wear coefficient conditions are shown in Figure 14(b).

From Figure 14(a), it can be seen that the wear coefficient has a large influence on the wear rate, and the larger the wear coefficient, the more drastic the occurrence of wear. When the wear coefficient is 1×10^{-6}, the armature wear volume is only 1.975 mm^3; when the smoothness of the pivot rail contact surface is reduced and the wear coefficient is 1×10^{-3}, the armature wear volume reaches 372.83 mm^3, which is about 190 times of the wear coefficient for. From the partial enlargement of Figure 14(a), it can be seen that the wear coefficient has little effect on the armature motion speed in the armature start-up section, although the effect of the wear coefficient on the armature motion speed is also very small at the 0.5ms moment. Combining Figure 14(a) and Figure 14(b), it can be seen that the larger the wear coefficient, the worse the contact condition, the larger the armature wear volume, and the smaller the armature motion speed subsequently.

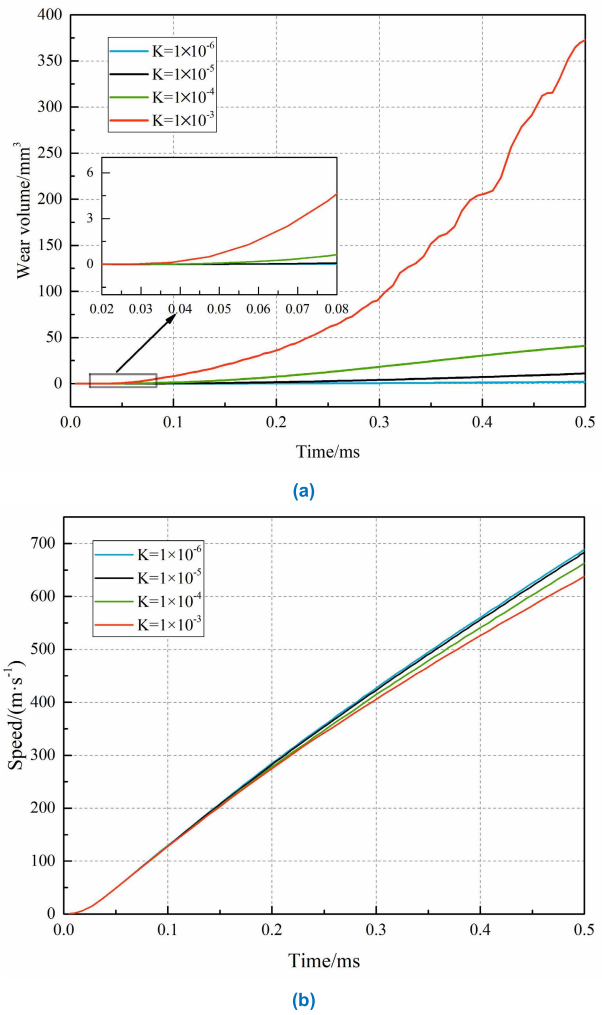

FIGURE 14. Influence of wear coefficient on wear characteristics: (a) Wear volume variation curve with time; and(b) Velocity versus time curve.

The wear is influenced by the wear coefficient, so in the process of engineering application, in order to reduce the wear of armature and rails and prolong the rails life, the process level of armature and rail should be improved as much as possible and the lubrication condition between armature and rail should be improved.

V. CONCLUSION

In this paper, a finite element simulation method for electromagnetic rail gun wear prediction is proposed, and some conclusions with theoretical and engineering application value

are obtained through the study of electromagnetic railgun launch test and friction wear, which have practical significance for extending the service life and engineering application of electromagnetic rail launcher.

(1) The wear between the support rails has a great influence on the stability of the launch, especially at high speed and heavy load (overfilling contact). According to the analysis of contact and wear characteristics, it can be seen that the wear of the frictional pair is proportional to the load, which is in accordance with Archard wear theory.

(2) The wear of the electromagnetic rail launcher during a single launch occurs mainly on the armature, and the tail of the armature arm is severely worn, which is mainly determined by the high current and strong contact load during the launch. The simulation results are consistent with the experimental verification results, which verifies the effectiveness of the wear simulation method.

(3) With the increase of electromagnetic thrust, the increase of armature wear does not change much and is approximately equal; the armature wear is greatly influenced by the wear coefficient. When the wear coefficient increases from 1×10^{-6} to 1×10^{-3}, the armature wear increases about 190 times. Therefore, in order to reduce the wear between the pivot guides, the lubrication conditions should be improved as much as possible.

REFERENCES

[1] W. M. Ma, J. Y. Lu, and X. P. Li, "Electromagnetic launch hypervelocity integrated projectile," *J. Nat. Univ. Defense Technol.*, vol. 41, no. 4, pp. 1–10, 2019.

[2] L. Gharib and A. Keshtkar, "Electromagnetic interference of railgun and its effect on surrounding electronics," *IEEE Trans. Plasma Sci.*, vol. 47, no. 8, pp. 4196–4202, Aug. 2019.

[3] R. Ciolini, M. Schneider, and B. Tellini, "The use of electronic components in railgun projectiles," in *Proc. 14th Symp. Electromagn. Launch Technol.*, Jun. 2008, pp. 1–6.

[4] S.-D. Ren, G. Feng, T.-D. Li, and H. Yang, "Analysis of electromagnetic characteristics of a new electromagnetic ejection device," *J. Phys., Conf.*, vol. 1939, no. 1, May 2021, Art. no. 012021.

[5] H. Li, "Structural parameter analysis of electromagnetic railgun barrel under heavy load," Ph.D. dissertation, Nanjing Univ. Sci. Technol., Nanjing, China, 2011.

[6] L. Lin, Y. Zhao, and W. Yuan, "Thermal effect analysis of railgun tests under transient conditions," *High Voltage Eng.*, vol. 42, no. 9, pp. 2864–2869, Sep. 2016.

[7] L. Dong, "Study on current carrying friction and wear mechanism," Ph.D. dissertation, Southwest Jiaotong Univ., Chengdu, China, 2008.

[8] Z. Chunyan, W. Jun, M. Fuqiang, N. Yanjie, T. Bo, and L. Baoming, "Analysis of sliding electric contact characteristics of series-augmented railgun based on breech voltage," *Acta Armamentarii*, vol. 41, no. 7, pp. 1280–1287, Jul. 2020.

[9] T. F. Fan, S. U. Zizhou, F. A. Tianfeng, Z. H. Tao, Z. H. Honghai, and L. I. Yong, "Geometry design and contact force analysis of C-shaped monolithic armature," *Acta Armamentarii*, vol. 40, no. 10, pp. 1969–1976, 2019.

[10] T. Y. Zhang, B. Q. Mao, and X. H. Bai, "Effect of plasma on ablation wear and fatigue life of inner wall of electromagnetic railgun," *J. Ordnance Equip. Eng.*, vol. 41, no. 7, pp. 33–37, 2020.

[11] B. Li, "Analysis of force load on the rail in rapid-fire mode of electromagnetic rail launcher," *Acta Armamentarii*, vol. 39, no. 3, pp. 618–624, 2018.

[12] T. Yan, L. I. U. Guimin, Z. H. U. Shuo, D. U. Linfei, and H. U. I. Yang, "Current research status of electromagnetic rail materials surface failure and strengthen technology," *Mater. Rep.*, vol. 32, no. 1, pp. 135–140, 2018.

[13] T. G. Lu, "Wear characteristics between armature and rails under the action of Lorentz force and temperature field," *Tribology*, vol. 41, no. 4, pp. 474–483, 2021.

[14] I. L. Singer, M. J. Veracka, C. N. Boyer, and J. M. Neri, "Wear behavior of lubricant-conditioned copper rails and armatures in a railgun," *IEEE Trans. Plasma Sci.*, vol. 39, no. 1, pp. 138–143, Jan. 2011.

[15] J. Wu, G. Wan, N. Cheng, L. Li, and B. Li, "Research on armature's wearing and dynamic interior ballistic of a railgun," *IEEE Trans. Plasma Sci.*, vol. 45, no. 7, pp. 1202–1207, Jul. 2017.

[16] D. G. Bansal and J. L. Streator, "Behavior of copper-aluminum tribological pair under high current densities," in *Proc. 14th Symp. Electromagn. Launch Technol.*, Jun. 2008, pp. 1–6.

[17] X. Gao, "Analysis on wear characteristics of pivot rail of electromagnetic railgun," Ph.D. dissertation, Yanshan Univ., Qinhuangdao, China, 2020.

[18] C. L. Gui, "The Archard design calculation model and its application method," *Lubrication Eng.*, vol. 1, pp. 12–21, Jun. 1990.

[19] C. Persad and Z. Castro, "Railgun tribology: Characterization and control of multishot wear debris," *IEEE Trans. Magn.*, vol. 43, no. 1, pp. 173–177, Jan. 2007.

[20] Z. Xiao, "Study on friction and wear of armature rail current carrying sliding contact surface," Ph.D. dissertation, Huazhong Univ. Sci. Technol., Wuhan, China, 2012.

[21] J. F. Archard, "Contact and rubbing of flat surfaces," *J. Appl. Phys.*, vol. 24, no. 8, pp. 981–988, 1953.

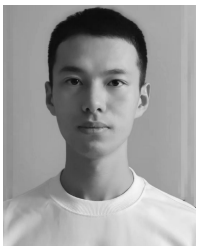

SHIDA REN was born in Jilin, China, in 1997. He is currently pursuing the master's degree in the theory of electromagnetic launch technology with Air Force Engineering University, Xi'an, China. His current research interests include the theory of electromagnetic rail launchers and numerical analysis of electromagnetic fields.

GANG FENG was born in Shaanxi, China, in 1976. He received the M.S. degree in weapons from Air Force Engineering University, Xi'an, China. He is currently an Associate Professor with the Air and Missile Defense College, Air Force Engineering University. His current research interest includes the theory and technology of weapons.

SHAOWEI LIU was born in Shaanxi, China, in 1979. He received the B.S. and Ph.D. degrees in weapons from Air Force Engineering University, Xi'an, China, in 2005 and 2008, respectively. He is currently an Associate Professor with the School of Air Defense and Missile Defense, Air Force Engineering University. His current research interest includes theory and technology of weapon systems.